Clinical Chemistry 46:7
976–988 (2000)

Nutrition

Identification of Lignans as Major Components in the Phenolic Fraction of Olive Oil

Robert W. Owen,[1*] Walter Mier,[2] Attilio Giacosa,[3] William E. Hull,[4]
Bertold Spiegelhalder,[1] and Helmut Bartsch[1]

Background: **Because olive oil is an important component of the Mediterranean diet, it is necessary to establish unequivocal identification of the major potential antioxidant phenolic compounds it contains.**
Methods: **The major phenolic antioxidants in extra virgin olive oil were isolated and purified. Structural analysis was conducted using several spectroscopic techniques, including mass spectrometry and nuclear magnetic resonance (NMR). In particular, detailed ^{1}H and ^{13}C NMR data are presented, and several assignment errors in the literature are corrected.**
Results: **The data show for the first time that the lignans (+)-1-acetoxypinoresinol and (+)-pinoresinol are major components of the phenolic fraction of olive oils. These lignans, which are potent antioxidants, are absent in seed oils and virtually absent in refined virgin oils but are present at concentrations of up to 100 mg/kg (mean ± SE, 41.53 ± 3.93 mg/kg; range, 0.65–99.97 mg/kg) in extra virgin oils. As with the simple phenols and secoiridoids, there is considerable interoil variation in lignan concentrations. Foods containing high amounts of lignan precursors have been found to be protective against breast, colon, and prostate cancer.**
Conclusion: **Lignans, as natural components of the diet, may be important modulators of cancer chemopreventive activity.**

The Mediterranean diet with its high content of fruits, vegetables, fiber, fish, and olive oil represents a healthy and disease-preventive diet *(1)*. Its protective effect appears quite broad in that it not only has a chemoprotective effect against cancer (especially of the colorectum and breast) but also significantly reduces mortality from heart disease *(2, 3)*.

Recent data suggest that the components of dietary olive oil may have a greater role in disease prevention than previously thought *(4–8)*. Olive oil can be consumed in the natural unrefined state, known as extra virgin oil quality (VOQ),[5] or as a refined product. The refined product (Fig. 1) is made either from virgin oil and called refined virgin oil (RVO) or from solvent-extracted oil *(9)* and called refined husk oil (RHO).

Virgin and refined oils differ little in fatty acid composition (Table 1). Monounsaturated oleic acid ($C_{18:1}$) is the main component, but there are nutritionally relevant contributions from saturated palmitic acid ($C_{16:0}$) and the essential polyunsaturated linoleic acid ($C_{18:2}$), whereas only a small amount of linolenic acid ($C_{18:3}$) is present. The proportion of linoleic acid, which is especially prone to undesirable oxidation by several processes, tends to be higher in oils from the more southern and warmer regions of the Mediterranean compared with oils from other areas.

VOQ, RVO, and RHO differ slightly in composition if the minor components, which account for 1% of VOQ and ~3% of RHO, are considered *(10)*. The higher concentrations of minor components in RHO compared with VOQ and RVO are chiefly attributable to fatty acid derivatives of long-chain alcohols (waxes) and to triterpenic alcohols. Many of these compounds contribute to the classical flavor of the oil, and some are detrimental to the taste, imparting bitterness or a burning sensation *(11)*. The high stability (shelf life) of olive oil is partly attributable to its high content of oleic acid, which is less prone to oxidation than linoleic and linolenic acids. In addition, simple and complex phenolic compounds (tocopherols), including

[1] Division of Toxicology and Cancer Risk Factors, [2] Division of Molecular Toxicology, and [4] Central Spectroscopy Department, German Cancer Research Center, Im Neuenheimer Feld 280, D-69120 Heidelberg, Germany.
[3] National Institute of Cancer Research, 16132 Genoa, Italy.
*Author for correspondence. Fax 49-6221-42-3359; e-mail r.owen@dkfz-heidelberg.de.
Received March 28, 2000; accepted April 27, 2000.

[5] Nonstandard abbreviations: VOQ, extra virgin olive oil; RVO, refined virgin olive oil; RHO, refined husk olive oil; SID, secoiridoid; OLG, oleuropein glucoside; PLC, preparative thin-layer chromatography; UV, ultraviolet; HP, Hewlett-Packard; GC, gas chromatography; MS, mass spectrometry; ESI, electrospray ionization; NMR, nuclear magnetic resonance; and TMS, tetramethylsilane.

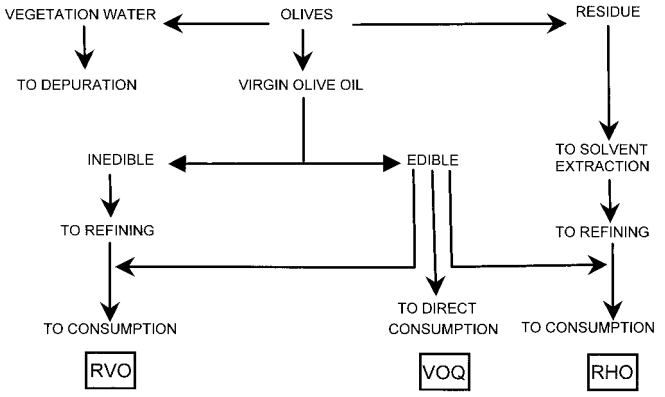

Fig. 1. Protocol for the extraction of various classes of olive oil.

vitamin E, provide a strong stabilizing effect *(12)*. Because refining causes a partial loss of antioxidants and their preservative actions, RVO and RHO usually are blended with a portion of VOQ to restore some of the desirable flavor and storage characteristics.

As part of our investigations into the chemopreventive effects of the Mediterranean diet, we considered it important to obtain a detailed profile of the major phenolic components in olive oil. To this end, we have studied a range of olive oils in comparison with seed oils to evaluate not only their compositions but also the antioxidative capacity of the major phenolic components *(13)*. We found that olive oils (especially extra virgin) contain, in addition to the previously identified simple phenols and secoiridoids (SIDs), two compounds belonging to the lignan class of phenolics. Here we describe the isolation, purification, and structural elucidation of these lignans and related phenolics (Figs. 2 and 3), using various analytical techniques.

Materials and Methods

REFERENCE COMPOUNDS

Authentic samples of the following compounds were purchased and used as references for structure elucidation: tyrosol (Sigma-Aldrich), and oleuropein glucoside (OLG; Extrasynthese Z.I. Lyon Nord). Acetic acid and methanol were obtained from E. Merck.

Table 1. Fatty acid profiles for three types of olive oils.[a]

Fatty acid	Fatty acid as % of total fatty acids
Oleic ($C_{18:1}$)	63.0–83.0
Palmitic ($C_{16:0}$)	7.0–17.0
Linoleic ($C_{18:2}$)	Maximum, 13.5
Stearic ($C_{18:0}$)	1.5–4.0
Palmitoleic ($C_{16:1}$)	0.3–3.0
Linolenic ($C_{18:3}$)	Maximum, 1.5
Others	Maximum, 3.0

[a] VOQ, RVO, and RHO.

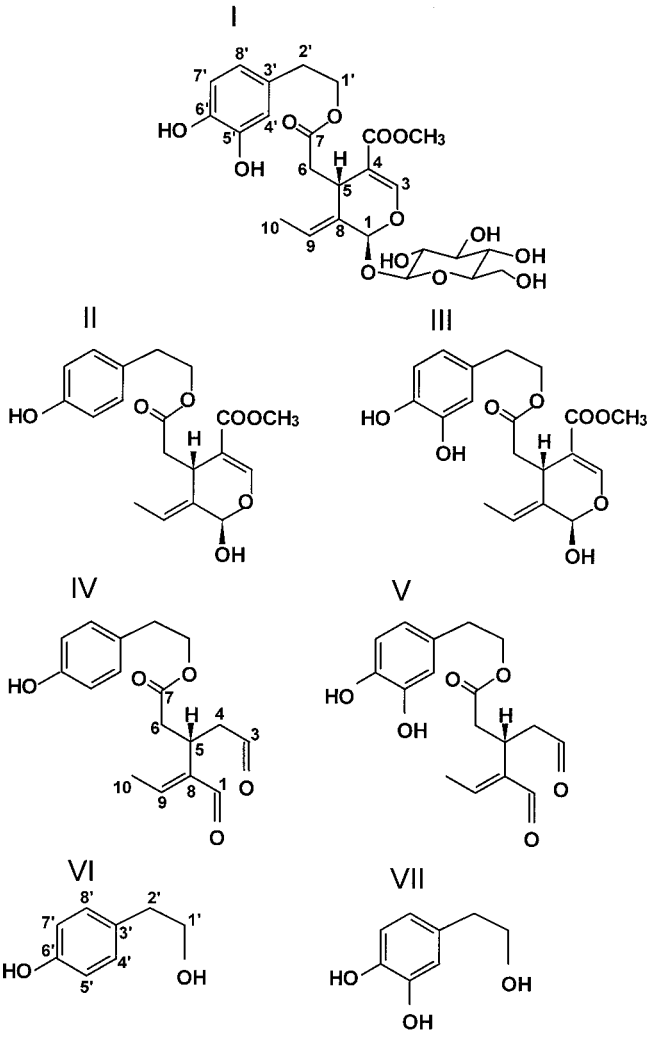

Fig. 2. Structures of OLG and related phenolic compounds.

I, OLG; ***II***, the aglycone of ligstroside; ***III***, oleuropein; ***IV*** and ***V***, the corresponding dialdehyde SIDs, which lack the carboxymethyl group at C4; ***VI***, tyrosol; ***VII***, hydroxytyrosol.

ORGANIC SYNTHESES

(3,4-Dihydroxyphenyl)ethanol (hydroxytyrosol; **VII**) was either synthesized according to a modification (the hydroxyl groups were not protected by acetylation) of the procedure of Papadopoulos and Boskau *(14)* or else obtained by acid hydrolysis of OLG. Acid hydrolysis was achieved by dissolving 100 mg of the glucoside in 1 L of 0.5 mol/L H_2SO_4 and incubating at 37 °C for 3 h. The hydrolysate was extracted twice with 250 mL of ethyl acetate and dried over anhydrous magnesium sulfate; the solvent was removed under reduced pressure. Hydroxytyrosol was purified by semipreparative HPLC to give an oily residue as the chromatographically and spectroscopically pure product.

EXTRACTION OF OIL

An olive oil (olio di oliva extravergine "ligustro" prodotto e confezionato dalla carapelli firenze s.p.a. via b. cellini 75

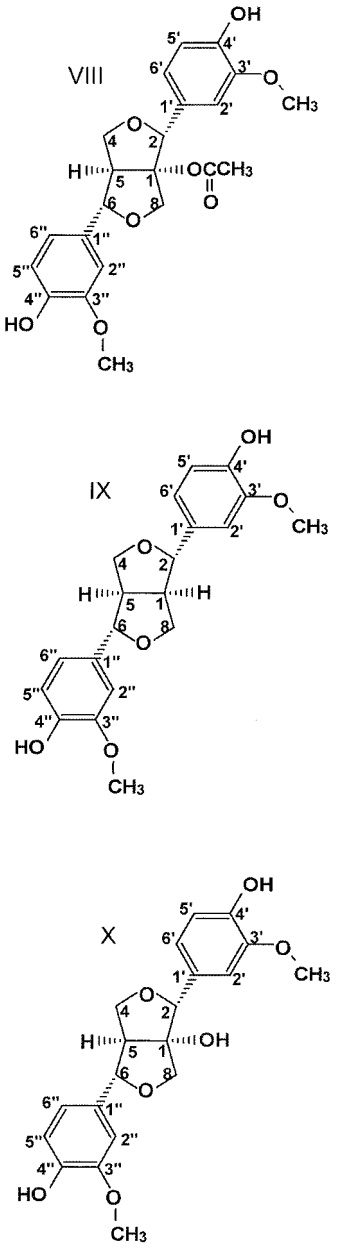

Fig. 3. Structures of the lignans (+)-1-acetoxypinoresinol (***VIII***), (+)-pinoresinol (***IX***), and (+)-1-hydroxypinoresinol (***X***).

tavarnelle val di pesa) known to contain considerable quantities of linked phenols *(13)* was chosen for the isolation of sufficient quantities of these substances for detailed analytical and spectroscopic analyses.

The oil (500 g) was extracted three times with methanol (100 mL) for 1 h with vigorous shaking (5000 rpm). The methanol extracts were pooled, and the solvent was removed under reduced pressure at 35 °C. The residue was resuspended in acetonitrile (50 mL) and extracted three times with hexane (50 mL) to remove lipid components. The hexane extracts were discarded, and the acetonitrile solution was dried over anhydrous magnesium sulfate. The acetonitrile was removed under reduced pressure (35 °C), and the dried residue was resuspended in methanol (1.0 mL).

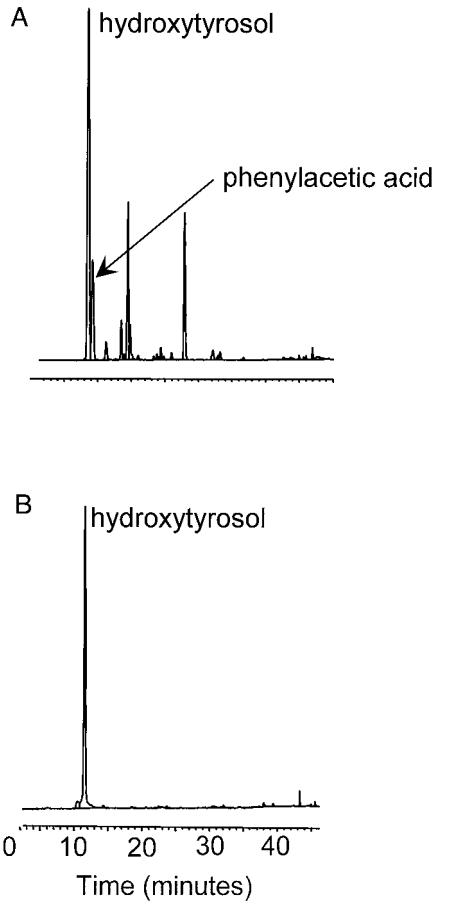

Fig. 4. HPLC chromatograms of hydroxytyrosol produced from 3,4-dihydroxyphenyl acetic acid (*A*) and OLG (*B*).

PREPARATIVE THIN-LAYER CHROMATOGRAPHY

Preparative thin-layer chromatography (PLC) was conducted on glass plates (20 × 20 cm) precoated with silica gel 50 F_{254} (Machery-Nagel). The extract (100 μL) was applied to the origins of 10 plates, and these were developed in the mobile phase ethyl acetate-isooctane-acetic acid (45:45:10, by volume). Bands on the thin-layer chromatography plates were detected under ultraviolet (UV) light (254 nm), and where relevant were scraped from the plates, pooled, and extracted three times with ethyl acetate. Solvent was removed under reduced pressure, and the extracts were resuspended in methanol (500 μL) for semipreparative HPLC.

HPLC

Analytical HPLC was conducted on a Hewlett-Packard (HP) 1090 liquid chromatograph under computer control (HP Chemstation operating under Microsoft® Windows™) using a C_{18} (Latex), reversed-phase 25-cm (5 μm) column (4 mm i.d.) as described previously

(13, 15–17); semipreparative HPLC was conducted on a similar column (10 mm i.d.).

GAS CHROMATOGRAPHY–MASS SPECTROMETRY

Gas chromatography–mass spectrometry (GC-MS) analyses were performed using a HP 5970 quadrupole mass spectrometer coupled to a HP 5890 gas chromatograph as described previously *(13)*.

ELECTROSPRAY IONIZATION-MASS SPECTROMETRY

Electrospray ionization (ESI) mass spectra were recorded on a Finnigan MAT TSQ 7000 mass spectrometer using methanol solutions and both the positive- and negative-ion modes. Molecular masses were determined by analysis of the spectra in terms of the detected molecular and bimolecular ions and ion clusters including sodium.

NUCLEAR MAGNETIC RESONANCE SPECTROSCOPY

Nuclear magnetic resonance (NMR) spectra were recorded in $CDCl_3$ or CD_3OD solvent on Bruker AC-250 and AM-500 spectrometers (Bruker Analytik) at ^1H frequencies of 250.133 MHz (compounds **IV** and **VI**) and 500.135 MHz (compounds **I, V,** and **VII–X**), respectively, or ^{13}C frequencies of 62.896 and 125.759 MHz, using conventional one-dimensional Fourier transform techniques (one-dimensional ^1H, ^{13}C with broadband ^1H decoupling, ^{13}C DEPT) for all compounds. Detailed analysis of zero-filled, resolution-enhanced spectra (peak picking, integration, and multiplet analysis) was performed using Bruker's WIN-NMR software for PCs. ^1H and ^{13}C chemical shifts (δ) are reported in ppm relative to the internal standard tetramethylsilane (TMS; $\delta = 0$) in $CDCl_3$ ($\delta =$ 7.26 for ^1H, 77.02 for ^{13}C) or relative to residual CHD_2OD ($\delta = 3.30$ ppm for ^1H) or CD_3OD (49.0 for ^{13}C), whereas H,H scalar couplings (J) are given in Hz. Most signal assignments could be made directly on the basis of the ^1H multiplet patterns, the carbon multiplicities (DEPT), and chemical shift predictions made using the empirical increment rules of SpecTool (Ver. 2.1; Chemical Concepts) and the ^{13}C data bank (22000 measured spectra) in Bruker's WIN-SpecEdit software, which uses hierarchically ordered spherical description of environment (HOSE) codes for carbon atom environments (substructures) to predict shifts from measured data. To resolve remaining assignment ambiguities, ^1H-coupled ^{13}C NMR spectra were obtained from compounds **I**, **V**, and **VII**, and the necessary selective ^1H decoupling experiments were performed. Finally, for the lignan **VIII,** two-dimensional NMR experiments [long-range H,H-correlation spectroscopy, ^1H-rotating frame Overhauser enhancement spectroscopy (ROESY), and one-bond C,H correlation] were performed using conventional pulse sequences.

HYDROLYSES

For acid hydrolysis of the crude extract and pure products, a 10-μL aliquot was transferred to a 15-mL glass centrifuge tube. Methanol was removed under a stream of nitrogen, and the residue was resuspended in 0.5 mol/L H_2SO_4 (100 μL) and incubated at 37 °C for 3 h on a shaking water bath. After incubation, the hydrolysates were extracted twice with ethyl acetate (2 mL). The pooled ethyl acetate extracts were dried under a stream of nitrogen and resuspended in methanol (100 μL). These solutions were used for analytical HPLC and, after derivatization with *bis*(trimethylsilyl)trifluoroacetamide, for GC-MS analysis.

Alkaline hydrolysis was conducted in a similar manner using 100 g/L KOH in methanol instead of 0.5 mol/L H_2SO_4. After incubation, the hydrolysates were diluted with distilled water (100 μL) and acidified to pH 2.0 with concentrated HCl and extracted as described above.

For large-scale alkaline hydrolysis, a delipidated extract of the oil (500 g) was resuspended in 100 g/L KOH in methanol (5.0 mL) and, after incubation and acidification, was extracted three times with ethyl acetate (25 mL). After removal of the solvent under reduced pressure, the hydrolyzed products were separated into crude fractions by PLC before purification by semipreparative HPLC.

Results

ISOLATION AND PURIFICATION OF OLIVE OIL COMPONENTS

Organic syntheses. Hydroxytyrosol (**VII**) was synthesized from 3,4-dihydroxyphenyl acetic acid by the method of Papadopoulos and Boskau *(14)*. HPLC (Fig. 4A) of the raw product mixture showed that the purity (yield) of hydroxytyrosol was ~50%, and this was confirmed by GC-MS (Table 2). The yield of hydroxytyrosol from the acid hydrolysis of OLG was essentially quantitative (Fig. 4B); therefore, this route is more convenient for the synthesis of this phenolic compound, which is not available commercially. A portion of the product (20 mg) was purified by preparative HPLC and analyzed by ^1H and ^{13}C NMR (see below).

Extraction of phenolic compounds. The HPLC chromatogram of the large-scale methanol extract of an extra virgin olive oil (500 g) is shown in Fig. 5. In the crude extract, seven major HPLC peaks (Fig. 5, peaks 1–4, 6, and 7) corresponded to the known compounds hydroxytyrosol (**VII**); tyrosol (**VI**); SID **V** and SID **IV**, which are dialdehydes related to oleuropein and ligstroside, respectively, but lacking the carboxymethyl group at C4 (as shown in Fig. 2); oleuropein (**III**); and the aglycone of ligstroside (**II**). Peak 5 in the HPLC chromatogram contained the lignans whose structures are shown in Fig. 3.

Other simple phenols that have been reported for extracts of olive oil (10 g) could not be detected routinely by HPLC, even when 100-g samples were extracted. However, during the preparative isolation of the major components by PLC, extraction of minor bands on the thin-layer chromatography plates and subsequent GC-MS analysis revealed that vanillic acid, *p*-hydroxybenzoic acid, *p*-coumaric acid, and *o*-coumaric acid were present

Table 2. GC-MS data (electron impact mode) for TMS derivatives of phenolic olive oil components.

Phenolic compound		TMS groups[a]	M^+	Major fragment ions, *m/z*
Ligstroside aglycone	**II**	2	506	192, 177
Oleuropein	**III**	3	594	280, 193
SID	**IV**	1	376	192, 177
SID	**V**	2	464	280, 193, 179
Tyrosol	**VI**	2	282	267, 193, 179, 103
Hydroxytyrosol	**VII**	3	370	355, 293, 267, 193, 179, 103
(+)-1-Acetoxypinoresinol	**VIII**	2	560	545, 351, 276, 245, 235, 223, 217, 209, 194, 187, 179, 131
(+)-Pinoresinol	**IX**	2	502	487, 403, 293, 235, 223, 209, 192, 179, 131
Hydroxypinoresinol	**X**	2	518	503, 492, 294, 279, 235, 225, 179, 131
		3[b]	590	575, 502, 366, 297, 224, 209, 194, 179, 127

[a] Each TMS group replaces a hydroxyl proton and adds 72 to the original molecular mass.
[b] TMS reaction performed overnight.

at very low concentrations, but their definitive quantification was not attempted. These findings are in agreement with the data of Angerosa et al. *(18)* but are contrary to that of Montedoro et al. *(15)*.

Acid hydrolysis of the methanol extract changed the HPLC profile dramatically (Fig. 6a). Both SIDs **IV** and **V** disappeared with concomitant increases in the concentrations of tyrosol and hydroxytyrosol, respectively. This is consistent with the hydrolysis of the ester group linking the elenolic acid and phenol moieties of the SIDs. HPLC peak 5 was unaffected by acid hydrolysis, indicating that the corresponding compound(s) did not possess the SID structure.

The HPLC chromatogram (Fig. 6B) after alkaline hydrolysis of the methanol extract yielded only tyrosol from SID **IV** (Fig. 6B, peak 2) because hydroxytyrosol from **V** is destroyed in strong alkaline solution. A new peak (Fig. 6B, peak 5b) appeared in the spectrum, whereas peak 5 (Fig. 6A) was appreciably diminished (Fig. 6B, peak 5a). These results suggested that two compounds were co-

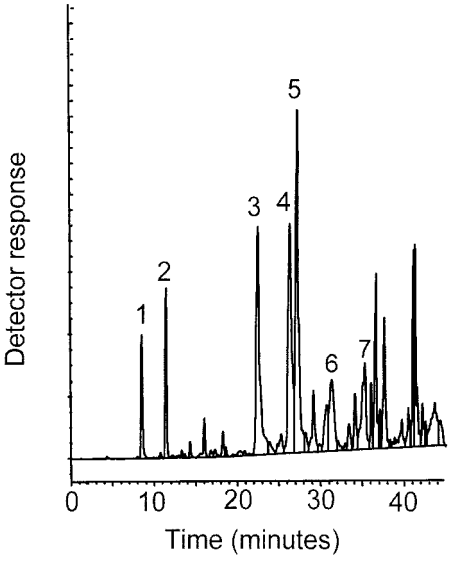

Fig. 5. HPLC chromatogram of a methanolic extract of an extra virgin olive oil.

Peaks: *1*, hydroxytyrosol (**VII**); *2*, tyrosol (**VI**); 3, SID (**V**); *4*, SID (**IV**); *5*, the lignans (+)-1-acetoxypinoresinol (**VIII**) and (+)-pinoresinol (**IX**); *6*, oleuropein (**III**); *7*, the aglycone of ligstroside (**II**).

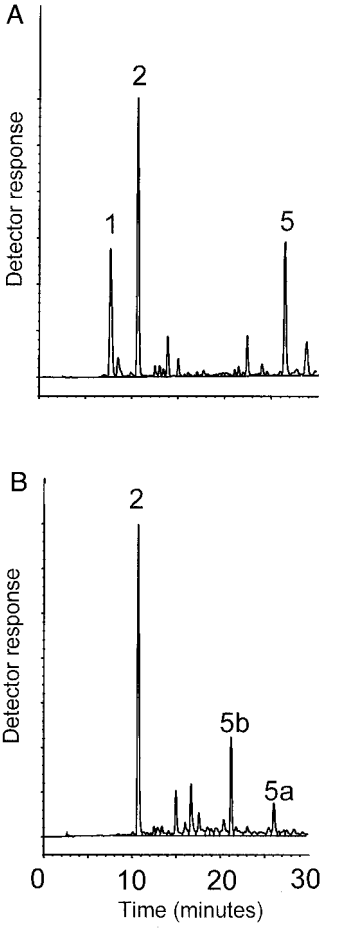

Fig. 6. HPLC chromatograms of a methanolic extract of an extra virgin olive oil after acid hydrolysis (*A*) and alkaline hydrolysis (*B*).

Peaks: *1*, hydroxytyrosol; *2*, tyrosol; *5*, the unresolved lignans (+)-pinoresinol and (+)-1-acetoxypinoresinol; *5a* and *5b*, the resolved lignans (+)-pinoresinol and (+)-1-hydroxypinoresinol, respectively.

Table 3. ESI-MS data (*m/z*) for phenolic olive oil components.

Phenolic compound		$[M-H]^-$	$[2M-H]^-$	$[M+H]^+$	$[M+Na]^+$	$[2M+Na]^+$
OLG	**I**	539	ND[a]	541	563	1103
Ligstroside aglycone	**II**	361	723	ND	385	747
Oleuropein	**III**	377	755	ND	401	ND
SID	**IV**	303	607	305	327	631
SID	**V**	319	639	321	343	663
Tyrosol	**VI**	137	275	139	161	ND
Hydroxytyrosol	**VII**	153	307	155	177	ND
(+)-1-Acetoxypinoresinol	**VIII**	415	831	417	439	855
(+)-Pinoresinol	**IX**	357	715	359	381	739
Hydroxypinoresinol	**X**	373	747	375	397	771

[a] ND, not detected.

chromatographing as peak 5 (confirmed by NMR), both resistant to acid hydrolysis and one resistant to alkaline hydrolysis.

PLC. PLC of the crude methanol extract yielded two fractions, and analytical HPLC showed that fraction 1 contained predominantly tyrosol (**VI**) and SID **IV**, whereas fraction 2 contained predominantly hydroxytyrosol (**VII**), SID **V**, and the lignans. This crude separation of **IV** (HPLC peak 4) from the lignans (HPLC peak 5) by PLC greatly facilitated subsequent purification by HPLC.

Purification of the PLC extracts by semipreparative HPLC gave the pure SIDs **IV** (10.0 mg) and **V** (9.0 mg). GC-MS and NMR analyses showed that the lignans (8.0 mg, corresponding to HPLC peak 5 in Fig. 5) were a mixture of a major and a minor compound, in agreement with the alkaline hydrolysis data. Analytical HPLC of PLC fraction 2 indicated that the minor component (~17.5%) was concentrated in the trailing edge of the lignan HPLC peak (chromatogram not shown). This facilitated further cycles of purification, giving the major component (**VIII**) in pure form but reduced yield (2.0 mg).

Alkaline hydrolysis of the methanol extract followed by PLC and preparative HPLC led to the isolation of the minor component (HPLC peak 5a, **IX**, 2.0 mg) and the alkaline hydrolysis product of the major component (HPLC peak 5b, **X**, 4.0 mg).

These lignans were found to be absent in seed oils and virtually absent in refined virgin olive oils, but they could

Table 4. ^{1}H NMR chemical shift data for tyrosol, hydroxytyrosol, the SIDs, and OLG.[a]

Position	Tyrosol (VI in CD_3OD)	SID IV ($CDCl_3$)	Hydroxytyrosol (VII in CD_3OD)	SID V ($CDCl_3$)	OLG[b] (I in CD_3OD)
1′	3.674 (t)[c]	(*a*) 4.230 (dt)	3.665 (dd)	(*a*) 4.226 (dt)	(*a*) 4.198 (dt)
		(*b*) 4.177 (dt)		(*b*) 4.157 (dt)	(*b*) 4.098 (dt)
2′	2.704 (tt)	2.822 (tt)	2.653 (ddt)	(*a*) 2.78 (dt)	2.754 (tt)
				(*b*) 2.75 (dt)	
4′	7.017 (dt)	7.052 (dt)	6.642 (dt)	6.706 (d)	6.657 (dt)
5′	6.690 (d)	6.757 (d)			
7′	6.689 (d)	6.757 (d)	6.666 (d)	6.778 (d)	6.684 (d)
8′	7.017 (dt)	7.052 (dt)	6.515 (ddt)	6.587 (dd)	6.539 (ddt)
1		9.238 (d)		9.197 (d)	5.896 (ddq)
3		9.634 (dd)		9.628 (dd)	7.497 (dd)
4		(*a*) 2.979 (ddd)		(*a*) 2.930 (ddd)	
		(*b*) 2.732 (ddd)		(*b*) 2.764 (ddd)	
5		3.610 (m)		3.622 (m)	3.960 (ddt)
6		(*a*) 2.689 (dd)		(*a*) 2.709 (dd)	(*a*) 2.690 (dd)
		(*b*) 2.605 (dd)		(*b*) 2.610 (dd)	(*b*) 2.431 (dd)
9		6.629 (q)		6.641 (q)	6.069 (qdd)
10		2.073 (d)		2.048 (d)	1.652 (dd)
$-CO_2Me$					3.701 (s)

[a] Chemical shifts at 30 °C are in ppm relative to TMS = 0 in $CDCl_3$ or relative to CHD_2OD = 3.30; basic multiplet type is given in parentheses; tyrosol and SID **IV** were measured at 250 MHz, the other compounds at 500 MHz.

[b] Shifts for the glucose moiety: H1, 4.796 (d); H2, 3.315 (dd); H3, 3.411 (dd); H4,H5, unresolved at 3.33 ppm; H6, (*a*) 3.876 (dd), (*b*) 3.668 (dd).

[c] t, triplet; dt, doublet-triplet; dd, doublet-doublet; tt, triplet-triplet; ddt, doublet-doublet-triplet; d, doublet; ddq, doublet-doublet-quartet; ddd, doublet-doublet-doublet; m, multiplet; q, quartet; s, singlet.

be isolated at concentrations of up to 100 mg/kg (mean ± SE, 41.53 ± 3.93; range, 0.65–99.97 mg/kg; n = 18) in extra virgin oils. As for the simple phenols and SIDs, we found considerable interoil variation in lignan concentrations.

STRUCTURE ELUCIDATION BY MS AND NMR

Simple phenols and SIDs. The structures of the simple phenols and SIDs are shown in Fig. 2, and mass spectra data (peak lists) for the phenolic olive oil components of interest are summarized in Tables 2 and 3. The GC-MS spectra (not shown) obtained from TMS derivatives of tyrosol (**VI**), hydroxytyrosol (**VII**), and SIDs **IV** and **V** are identical with those published previously *(18, 19)*. The molecular masses were further confirmed by ESI-MS data after taking into account possible cluster formation.

The ^{1}H and ^{13}C NMR data for hydroxytyrosol and tyrosol, SIDs **IV** and **V**, and for OLG (**I**) are given in Tables 4–6. Signal assignments were made using the numbering scheme shown in Fig. 2. Montedoro et al. *(17)* have also published ^{1}H and ^{13}C NMR data for these compounds, and their ^{13}C chemical shifts agree very closely with our values for all compounds. However, in their study, Montedoro et al. *(17)* gave an incorrect ^{1}H chemical shift for H8′ of tyrosol, which should be equivalent by symmetry with H4′, and they interchanged the assignments for C4′,8′ and C5′,7′ for tyrosol and the related SID **IV**. This latter error is clearly revealed by chemical shift predictions, which give 129–131 and 115–116 ppm for C4′ and C5′, respectively (observed: 130.86 and 116.13 for tyrosol; 130.2 and 115.3 for *p*-hydroxytoluene). Finally, the assignments for C2′ and C6 in SID **IV** remained ambiguous based on chemical shift predictions. Therefore, we confirmed the assignments made by Montedoro et al. *(17)* by performing selective ^{1}H decoupling experiments (see below).

For hydroxytyrosol (**VII**) two pairs of ^{13}C assignments were ambiguous at the level of chemical shifts alone. The quaternary carbons C5′ and C6′ exhibited shifts near 146 ppm with a shift difference of 1.5 ppm. Shift predictions by increments rules suggested that C5′ should have the larger shift value, whereas Montedoro et al. *(17)* assigned C6′ to the larger shift without providing convincing proof. Similarly, the protonated carbons C4′ and C7′ gave resonances near 117 ppm with a shift difference of only 0.8 ppm. Shift predictions generally suggested that C7′ should have the larger shift, as assigned by Montedoro et al. *(17)*. To resolve these ambiguities, we measured the fully ^{1}H-coupled ^{13}C spectrum of hydroxytyrosol and

Table 5. ^{1}H NMR coupling constant data for tyrosol, hydroxytyrosol, the SIDs, and OLG.[a]

Coupling	Tyrosol (VI in CD_3OD)	SID IV ($CDCl_3$)	Hydroxytyrosol (VII in CD_3OD)	SID V ($CDCl_3$)	OLG[b] (I in CD_3OD)
$^{2}J_{1'a,1'b}$	−10.9[a]	−10.77	−10.5[d]	−10.82	−10.71
$^{2}J_{2'a,2'b}$	−13.8[c]		−13.4[d]	−14.2	
$^{3}J_{1',2'}$	6.4; 8.0[c]	7.08 (1′a)	6.33; 8.18[d]	6.71 (1′a)	7.02 (1′a)
		6.90 (1′b)		6.49 (1′b)	7.10 (1′b)
$^{4}J_{2'4'}$	0.61	0.66	0.54		0.56
$^{4}J_{2',8'}$	0.61	0.66	0.54		0.53
$^{3}J_{4',5'}$	8.27[e]	8.25[e]			
$^{3}J_{7',8'}$	8.27	8.25	8.02	8.07	8.01
$^{4}J_{4',8'}$	2.14	2.13	2.07	1.90	2.05
$^{4}J_{5',7'}$	2.84	2.95			
$^{5}J_{4',7'}$	0.38	0.38			
$^{4}J_{1,5}$		2.00		1.93	$^{4}J_{1,3}$ = 0.59
					$^{4}J_{1,9}$ = 1.50
					$^{5}J_{1,10}$ = 1.55
$^{3}J_{3,4a}$		1.32		1.23	$^{4}J_{3,5}$ = 0.70
$^{3}J_{3,4b}$		0.98		0.96	
$^{2}J_{4a,4b}$		−18.26		−18.36	$^{4}J_{5,9}$ = 0.58
$^{3}J_{4a,5}$		8.58		8.24	
$^{3}J_{4b,5}$		5.61		5.83	
$^{2}J_{6a,6b}$		−15.94		−15.7	−14.08
$^{3}J_{5,6a}$		8.04		8.68	4.58
$^{3}J_{5,6b}$		6.95		6.49	9.11
$^{3}J_{9,10}$		7.08		7.10	7.13

[a] See footnote *a* in Table 4; except where noted, couplings in Hz were determined by first-order analysis; the signs of geminal and vicinal couplings are assumed to be negative and positive, respectively; the signs of long-range couplings have not been determined.

[b] Resolved couplings for the glucose moiety: $^{3}J_{1,2}$ = 7.70; $^{3}J_{2,3}$ = 9.2; $^{3}J_{3,4}$ = 8.8; $^{2}J_{6a,6b}$ = −11.95; $^{3}J_{5,6a}$ = 1.92; $^{3}J_{5,6b}$ = 5.57.

[c] Observed pseudo-triplet splitting for H1′ was 7.2 Hz; data in Table 5 were calculated by AA′XX′ spin system analysis of the H1′ multiplet.

[d] Observed dd splittings for H1′ were 6.99 and 7.49 Hz; data in Table 5 were calculated by AA′XX′ spin system analysis of the H1′ multiplet.

[e] The couplings for H4′–H8′ were obtained by AA′XX′ spin system analysis; the observed pseudo-doublet splitting for H4′,8′ and H5′,7′ was 8.69 Hz for tyrosol and 8.64 for SID **IV**.

Table 6. ^{13}C NMR data for tyrosol, hydroxytyrosol, the SIDs, and OLG.[a]

Position	Tyrosol (VI in CD_3OD)	SID IV ($CDCl_3$)	Hydroxytyrosol (VII in CD_3OD)	SID V ($CDCl_3$)	OLG[b] (I in CD_3OD)
1′	64.58 (t)[c]	65.15 (t)	64.59 (t)	65.25 (t)	66.87 (t)
2′	39.41 (t)	34.19 (t)[d]	39.65 (t)	34.26 (t)[d]	35.39 (t)[d]
3′	131.04 (s)	129.86 (s)	131.80 (s)	130.44 (s)	130.76 (s)
4′	130.86 (d)[e]	130.05 (d)[e]	117.07 (d)[f]	116.22 (d)[f]	117.06 (d)[f]
5′	116.13 (d)[e]	115.37 (d)[e]	146.15 (s)[g]	143.60 (s)[g]	146.23 (s)[g]
6′	156.76 (s)	154.29 (s)	144.62 (s)[g]	142.79 (s)[g]	144.92 (s)[g]
7′	116.13 (d)	115.37 (d)	116.31 (d)[f]	115.33 (d)[f]	116.45 (d)[f]
8′	130.86 (d)	130.05 (d)	121.21 (d)	121.21 (d)	121.31 (d)
1		195.11 (d)		195.78 (d)	95.24 (d)
3		200.39 (d)		200.97 (d)	155.13 (d)
4		46.23 (t)		46.24 (t)	109.41 (s)
5		27.28 (d)		27.22 (d)	31.81 (d)
6		36.88 (t)[d]		36.99 (t)[d]	41.26 (t)[d]
7		171.92 (s)		172.02 (s)	173.20 (s)
8[h]		143.34 (s)		143.19 (s)	130.53 (s)
9[h]		154.23 (d)		155.17 (d)	124.86 (d)
10		15.25 (q)		15.29 (q)	13.53 (q)
$-\underline{C}O_2$ Me					168.68 (s)
$-CO_2$ <u>Me</u>					51.90 (q)

[a] Chemical shifts at 30 °C are relative to TMS = 0 ($CDCl_3$ = 77.014) or CD_3OD = 49.0; multiplicities in parentheses; tyrosol and SID **IV** were measured at 62.9 MHz, the other compounds at 125.76 MHz.

[b] Shifts for glucose moiety, C1–C6; 100.92, 74.76, 77.94, 71.47, 78.41, 62.73.

[c] t, triplet; s, singlet; d, doublet; q, quartet.

[d] Assignments according to Montedoro et al. *(17)* were unequivocally confirmed in this work.

[e] Assignments here are based on reference data from analogous compounds; erroneously reversed in Montedoro et al. *(17)*.

[f] In Montedoro et al. *(17)*, the assignments for C4′,C7′ are reversed; our assignments were unequivocally confirmed by long-range ^{1}H couplings for C4′: ^3J(H2′) = 5.2; ^3J(H8′) = 7.4; ^4J(H7′) = 1.2.

[g] In Montedoro et al. *(17)*, the assignments for C5′,C6′ are reversed; our assignments were unequivocally confirmed by ^{1}H-coupled spectra and selective decouplings; e.g., the observed diagnostic long-range ^{1}H couplings are ^2J(H4′) = 3.2; ^3J(H7′) = 7.1; ^4J(H8′) = 1.2 for C′5; and ^2J(H7′) = 3.0; ^3J(H4′) = 6.7; ^3J(H8′) = 9.7 for C′6.

[h] The numbering scheme for C8,C9 is the reverse of that used by Montedoro et al. *(17)*.

performed appropriate selective ^{1}H decoupling experiments. The long-range CH coupling patterns in the aromatic ring are unique for each site, following the rule $^3J > {}^2J > {}^4J$. Thus, the assignments given in Table 6 are unambiguous (footnotes to Table 6 for diagnostic coupling constants), and correct the earlier erroneous assignments *(17)*.

For SID **V** and OLG (**I**), fully coupled and selectively decoupled ^{13}C NMR spectra were also obtained to resolve all ambiguities involving the hydroxytyrosol ring carbons, the olefin carbon C8 and the methylene carbons C2′ and C6. The results are summarized in Table 6 and its footnotes.

Our ^{1}H NMR analysis agrees with most of the results and assignments obtained by Montedoro et al. *(17)* at lower magnetic field strength. There are some differences in the absolute values of chemical shifts for the aromatic protons, but the order of shifts and their assignments agree with our results. However, at a higher field and with resolution enhancement we were able to resolve a variety of long-range couplings and the following nonequivalent methylene protons: H1′a,b in OLG and the SIDs; H2′a,b in SID **V**; H4a,b in SIDs **IV** and **V**; H6a,b in OLG and the SIDs. The assignments given by Montedoro et al. *(17)* for H4a,b and H6a,b and their geminal couplings are incorrect.

Lignans. The structures of the lignans are shown in Fig. 3, and the NMR data are summarized in Tables 7–9. The one-dimensional ^{1}H and ^{13}C NMR spectra of **VIII** are depicted in Fig. 7.

[+]-1-Acetoxypinoresinol (VIII). The UV spectrum indicated the presence of a phenolic compound [λ_{max}, nm (log ϵ): 230 (3.94), 279 (3.37)]. The ESI mass spectrum (Table 3) afforded a signal for $[M+H]^+$ at *m/z* 417, consistent with the molecular formula $C_{22}H_{24}O_8$ (exact mass, 416.147). Formation of the trimethylsilyl derivative (GC-MS spectrum in Fig. 8A) led to an increase of the molecular mass by 144 units, indicating the presence of two free hydroxyl groups (Table 2). Whereas acidic hydrolysis exerted no effect, alkaline hydrolysis led to a product (**X**) with similar UV characteristics [λ_{max}, nm (log ϵ): 232 (4.16), 280 (3.73)] and a molecular mass of 374

Table 7. ^{1}H NMR chemical shift data for the lignans in $CDCl_3$.[a]

Position	(+)-Pinoresinol (C_2-symmetry) IX	(+)-1-Hydroxy-pinoresinol X	(+)-1-Acetoxy-pinoresinol VIII
1	3.099 (m)[b]		
2	4.738 (d, br)	4.852 (br, s)	5.064 (br, s)
4a	4.247 (dd)	4.534 (dd)	4.424 (dd)
4b	3.879 (dd)	3.847 (dd)	3.775 (dd)
5	3.099 (m)	3.116 (ddd)	3.324 (dt)
6	4.738 (d, br)	4.864 (br, d)	4.745 (d)
8a	4.247 (dd)	4.060 (d)	4.435 (d)
8b	3.879 (dd)	3.92 (NR)	4.239 (d)
2′	6.897 (dm)	7.001 (dm)	6.850 (dm)
5′	6.890 (d)	6.902 (NR)	6.860 (NR)
6′	6.821 (ddd)	6.900 (NR)	6.856 (NR)
3′-OMe	3.908 (s)	3.907 (s)	3.894 (s)
2″	6.897 (dm)	6.982 (dm)	6.968 (dm)
5″	6.890 (d)	6.953 (d)	6.917 (dd)
6″	6.821 (ddd)	6.877 (ddd)	6.884 (ddd)
3″-OME	3.908 (s)	3.926 (s)	3.925 (s)
CH_3CO_2-			1.705 (s)

[a] Chemical shifts at 500 MHz and 30 °C in ppm relative to TMS = 0 in $CDCl_3$; multiplet type in parentheses.

[b] m, multiplet; d, doublet; br, broadened; s, singlet; dd, doublet-doublet; ddd, doublet-doublet-doublet; dt, doublet-triplet; NR, multiplet not resolved; dm, doublet-multiplet.

(Table 3), consistent with the replacement of one acetate group by a hydroxyl. This was corroborated by the GC-MS spectrum of the trimethylsilyl derivative, which gave a molecular mass of 518 (Fig. 9A) after short-term (15 min) and 590 (Fig. 9B) after overnight derivatization (Table 2).

The 500 MHz ^{1}H NMR spectrum of **VIII** (Fig. 7A) showed seven aliphatic protons at δ = 3.33–5.06 and singlets at δ = 1.703, 3.891, and 3.923, indicating the presence of an acetate ester and two aromatic methoxy groups. A total of six aromatic protons were detected in the range δ = 6.85–6.97. Three multiplets could be resolved, which showed the characteristic pattern of ortho and meta coupling constants (Table 8) for the three protons of 1,3,4 tri-substituted benzene rings (H2″, H5″, H6″ in Table 7) with an additional long-range coupling from H6″ to the aliphatic proton H6. For the second ring system, the multiplet for H2′ was resolved, but H5′ and H6′ had nearly identical chemical shifts and gave a nonclassical pattern of three closely spaced resonances. The chemical shifts for H5′ and H6′ were assigned via a two-dimensional C,H correlation experiment. The discrimination between the "prime" ring system attached to C2 and the "double prime" system attached to C6 was made easily via an H,H-correlation spectroscopy experiment performed with an evolution delay that detected the long-range couplings between H2′ and H2 and between H6 and H2″,5″,6″. At the same time, each 3-OMe group could be assigned via long-range coupling to the corresponding ring proton at the C2′ or C2″ position. On the basis of nuclear Overhauser effects observed via a two-dimensional ROESY experiment, we tentatively assign H2, H4b, H6, and H8b to pseudo-axial positions above the plane of Fig. 3.

Deacetylation of **VIII** by alkaline hydrolysis to give **X**

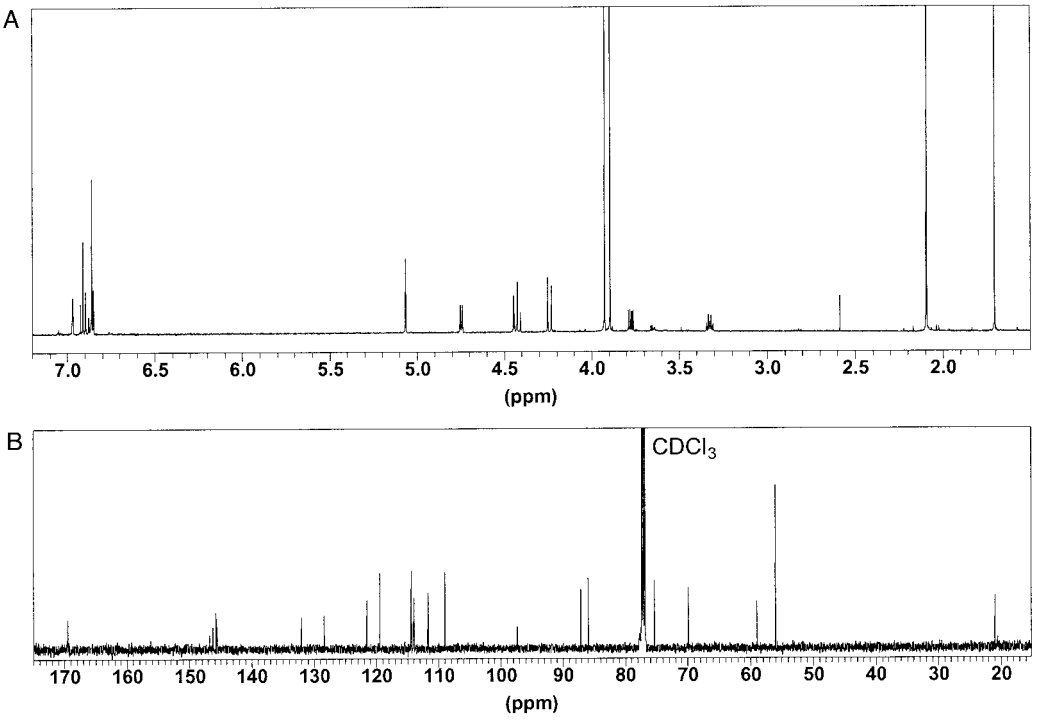

Fig. 7. ^{1}H NMR (500 MHz; *A*) and ^{13}C NMR (125 MHz; *B*) spectra of (+)-1-acetoxypinoresinol (**VIII**).

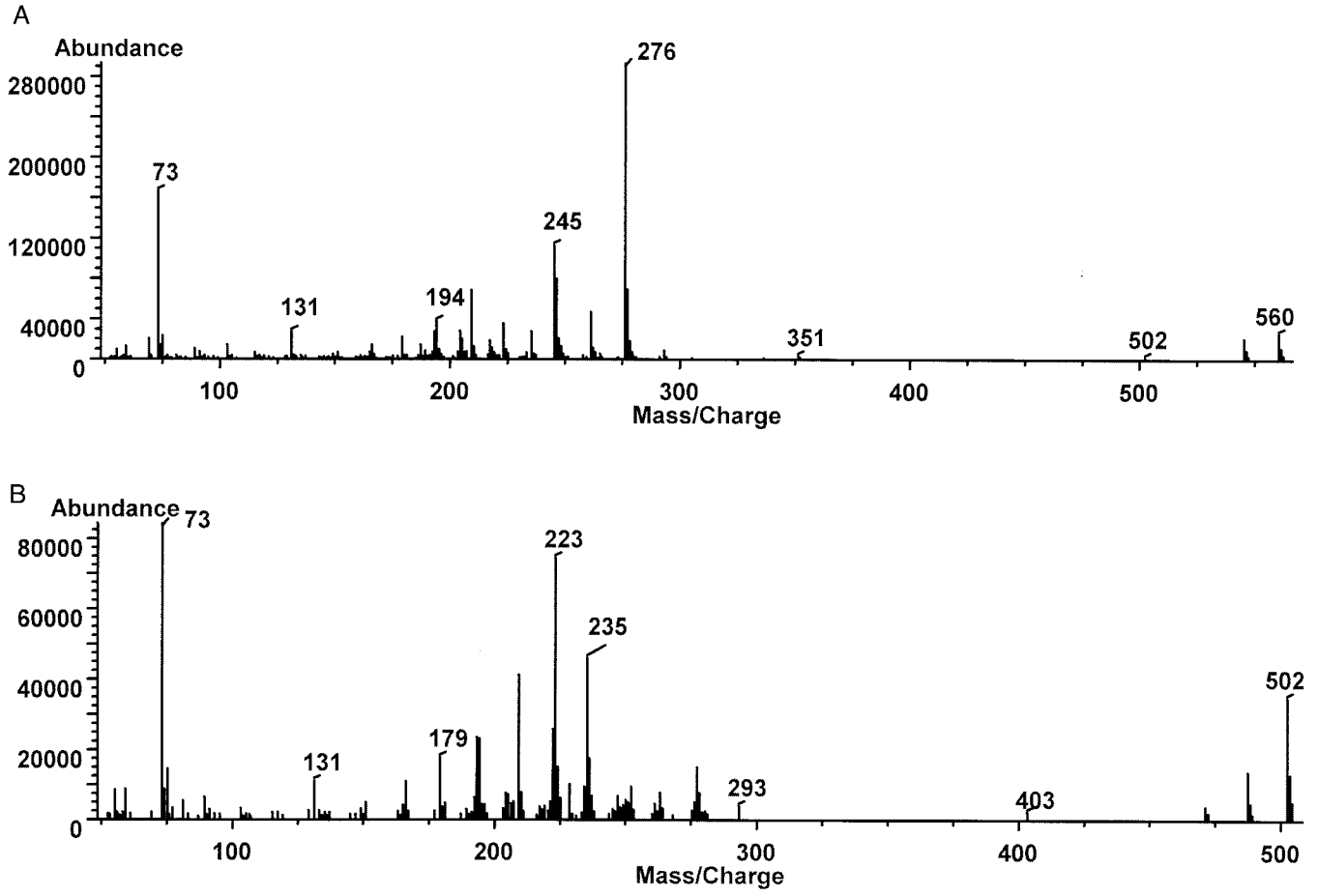

Fig. 8. GC-MS spectra of the TMS ethers of (+)-1-acetoxypinoresinol (**VIII**; *A*) and (+)-pinoresinol (**IX**; *B*).

produced upfield shifts for C1 and for the proton signals at 5.06, 4.44, 4.24, and 3.33 ppm; a substantial downfield shift was observed for one of the aromatic protons (H2′), and substantial changes in carbon shifts were observed only for the prime ring system. Putting all of this information together, we deduced that these compounds were lignans with a 2,6-diaryl-3,7-dioxabicyclo[3.3.0]octane skeleton with the prime aryl ring attached to C2 and the double prime ring attached to C6. The chemical shifts for the prime aryl ring and the protons at C2,5,8 are particularly sensitive to the substituent at C1.

With the C,H correlation data for **VIII,** unequivocal assignments for all protons and protonated carbons were obtained. Quaternary aryl carbons C1,3,4 were assigned via shift predictions. The only ambiguity remaining is the discrimination between C3′ and C3″ and between C4′ and C4″. In Table 9, we have made the assignments based on the assumption that there will be minimal perturbations in the chemical shifts for C3″,C4″ for the series **VIII–X**, whereas larger effects are expected for C3′,C4′.

On the basis of the above data, the structures of **VIII** and **X** were elucidated as (+)-1-acetoxypinoresinol and (+)-1-hydroxypinoresinol, respectively. ^{13}C NMR data (15 MHz) for these compounds in deuterated dimethyl sulfoxide (DMSO-d_6) have been reported earlier by Tsukamoto et al. *(20)*, and substantial absolute differences in chemical shifts (solvent effects) in comparison with our data are apparent. Nevertheless, our assignments in terms of the order of chemical shifts agree completely with the earlier work for **VIII** and differ only for C3′, C3″, and C5′,C5″ in **X**. Agrawal and Pathak *(21)* have tabulated ^{13}C reference data for a large number of lignans, including **IX** and **X**, whereby the chemical shifts of the carbons of the 3,7-dioxabicyclo[3.3.0]octane moiety are found to be diagnostic for its stereochemistry and substitution pattern. Our data for **X** show excellent agreement with the data for structures with the stereochemistry as shown in Fig. 3.

[+]-Pinoresinol (IX). The UV spectrum [λ_{max}, nm (log ϵ): 231 (4.18), 281 (3.82)] indicated the presence of a compound that was similar to both **VIII** and **X**. The ESI mass spectrum (Table 3) gave a molecular ion signal $[M+H]^+$ at *m/z* 359, consistent with the formula $C_{20}H_{22}O_6$. Trimethylsilylation yielded a molecular mass of 502 by GC-MS (Table 2 and Fig. 8B), indicating the presence of two free hydroxyl groups. The compound was stable to both alkaline and acid treatment. The NMR of **IX** (Tables 7–9) revealed the twofold symmetry of this compound.

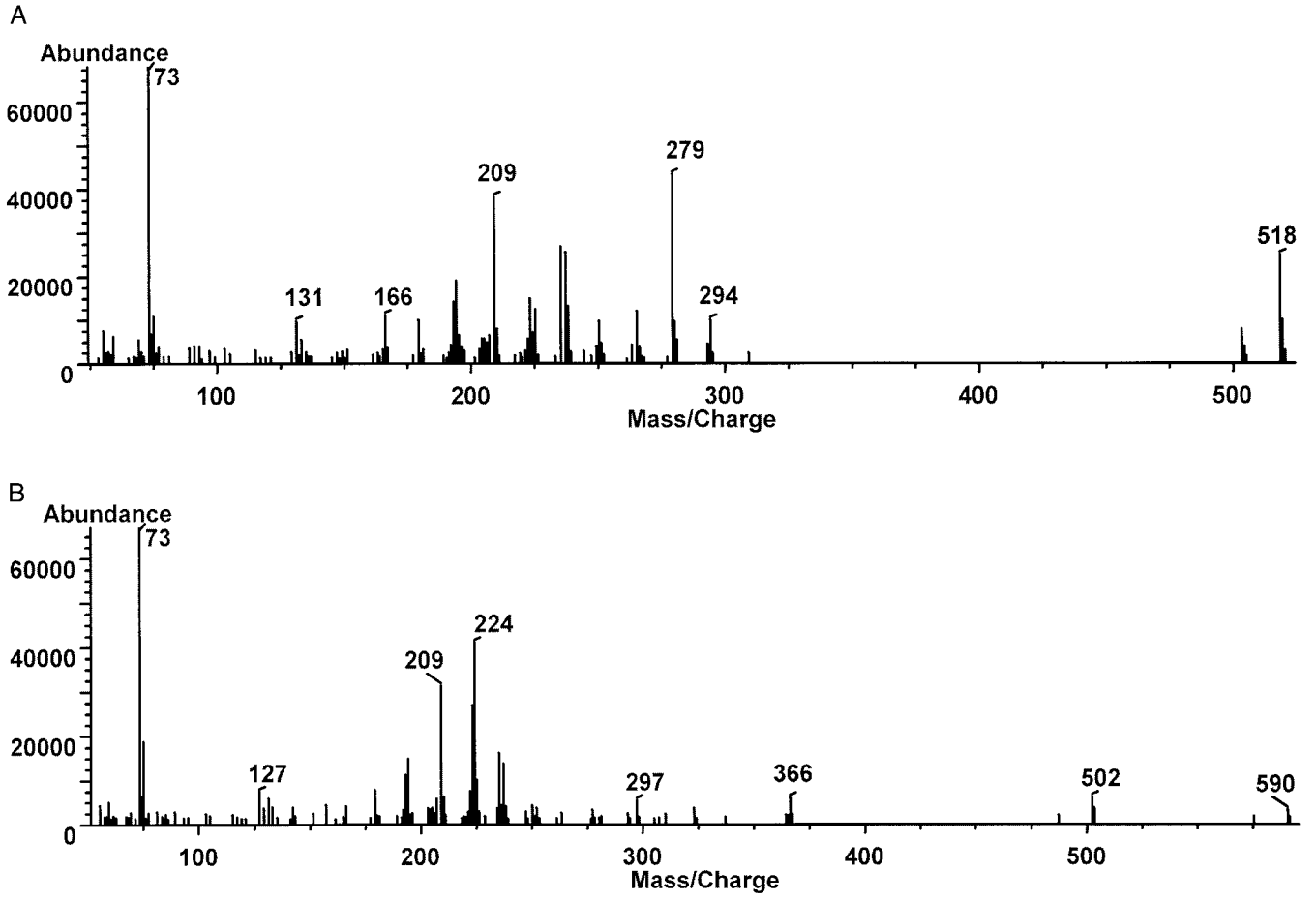

Fig. 9. GC-MS spectra of (+)-1-hydroxypinoresinol (**X**) after partial (two TMS ethers; *A*) and full (three TMS ethers; *B*) derivatization.

The close similarity of the spectra to those of **VIII** and **X** and the reference data of Agrawal and Pathak *(21)* indicated that **IX** is a symmetrical lignan with the 2,6-diaryl-3,7-dioxabicyclo[3.3.0]octane skeleton and stereochemistry shown in Fig. 3. Thus, we concluded that compound **IX** was (+)-pinoresinol, which has a C_2 axis perpendicular to the plane of Fig. 3.

Table 8. ^{1}H NMR coupling constants for the lignans in $CDCl_3$.[a]

Coupling	(+)-Pinoresinol IX	(+)-1-Hydroxy-pinoresinol X	(+)-1-Acetoxy-pinoresinol VIII
$^2J_{4a,b}$	−9.2	−9.19	−9.32
$^2J_{8a,b}$		−9.30	−10.81
$^3J_{4a,5}$	7.11	8.04	7.72
$^3J_{4b,5}$	3.85	6.33	4.80
$^3J_{5,6}$	4.81	4.9	5.02
$^4J_{2'',6''}$	2.00	1.88	1.88
$^3J_{5'',6''}$	8.17	8.12	8.12
$^4J_{6'',6}$	0.69	0.67	0.60

[a] Couplings in Hz at 500 MHz and 30 °C; the 2′,5′,6′ spin system was highly second order and could not be analyzed directly.

Discussion

The results of this study show for the first time that the lignans (+)-1-acetoxypinoresinol (**VIII**) and (+)-pinoresinol (**X**) are major components of the phenolic fraction of olive oils. In extra virgin oils, the quantity of lignans can be up to 100 mg/kg, but as with the simple phenols and SIDs, considerable interoil variation exists. The reasons for this probably lie in differences in the production areas, climate, olive varieties, and oil production techniques.

(+)-Pinoresinol is a common component of the lignan fraction of several plants such as *Forsythia* species *(22)* and *Sesamum indicum* seeds *(23)*, whereas (+)-1-acetoxypinoresinol and (+)-1-hydroxypinoresinol (**IX**) and their respective glucosides have been detected *(20, 24)* in the bark of the olive tree (*Olea europaea* L.). The question of how these lignans become a major component of the phenolic fraction of olive oil has yet to be answered. Recent studies (Owen et al., manuscripts in preparation) have shown that they are not present in the pericarp of the olive drupes, nor in the leaves and twigs that may be present in the mulch prepared for olive pressing. However, preliminary studies have shown that (+)-pinoresinol is a major component of the phenolic fraction of the

Table 9. ^{13}C NMR data for the lignans in $CDCl_3$ at 30 °C.[a]

Position	(+)-Pinoresinol (C_2-symmetry) IX	(+)-1-Hydroxy-pinoresinol X	(+)-1-Acetoxy-pinoresinol VIII
1	54.22 (d)[b]	91.71 (s)	97.31 (s)
2	85.91 (d)	87.82 (d)	87.12 (d)
4	71.71 (t)	71.69 (t)	69.87 (t)
5	54.22 (d)	60.17 (d)	58.90 (d)
6	85.91 (d)	85.86 (d)	85.90 (d)
8	71.71 (t)	74.78 (t)	75.29 (t)
1′	132.99 (s)	127.08 (s)	128.38 (s)
2′	108.64 (d)	109.40 (d)	111.63 (d)
3′	146.73 (s)[c]	146.99 (s)[d]	146.21 (s)[d]
4′	145.29 (s)[c]	146.09 (s)[d]	145.75 (s)[d]
5′	114.29 (d)	114.74 (d)	113.91 (d)
6′	119.00 (d)	119.72 (d)	121.46 (d)
3′-OMe	56.00 (q)	56.07 (q)	55.60 (q)
1″	132.99 (s)	132.46 (s)	132.00 (s)
2″	108.64 (d)	109.09 (d)	108.95 (d)
3″	146.73 (s)[c]	146.74 (s)[d]	146.77 (s)[d]
4″	145.29 (s)[c]	145.51 (s)[d]	145.57 (s)[d]
5″	114.29 (d)	114.32 (d)	114.36 (d)
6″	119.00 (d)	119.66 (d)	119.41 (d)
3″-OMe	56.00 (q)	55.98 (q)	55.60 (q)
$CH_3\underline{C}O_2-$			169.45 (s)
$\underline{C}H_3CO_2-$			20.92 (q)

[a] All measurements at 125.76 MHz (11.7 T) and 30 °C; chemical shift reference is TMS = 0 ($CDCl_3$ = 77.02) or CD_3OD = 49.0.

[b] d, doublet; s, singlet; t, triplet; q, quartet.

[c] Assigned by chemical shift predictions.

[d] Assigned assuming that C3″,C4″ will show minimal shift perturbations across the series **VIII–X**.

olive piths (Owen et al., manuscripts in preparation), and further information will be forthcoming from our ongoing studies.

Clearly, lignans constitute an important contribution to the phenolic fraction of olive oil and therefore may play a major role in the health promoting effects of the Mediterranean diet. The evidence for the chemopreventive effect of lignans is compelling. They are a group of compounds found only in plants, and a range of different classes have been described. Interest in lignans as possible chemopreventive agents began ~20 years ago when it was discovered that certain classes could be identified and quantified in biological material, especially human urine. The major lignans identified in humans are now termed enterolactone and enterodiol, and they are described as resulting from bacterial transformation in the large bowel of matairesinol and secoisolariciresinol, respectively *(25–27)*.

Lignans have been shown to inhibit skin, breast, colon, and lung cancer cell growth *(28, 29)* and to exert antiestrogenic effects. This is not surprising, considering the structural similarity between the lignans and the synthetic antiestrogen tamoxifen *(30, 31)*. Foods containing high amounts of lignan precursors have been found to be protective against breast cancer, in particular. Consumption of flaxseed, a concentrated source of lignans *(32)*, has been shown to inhibit mammary tumor promotion *(33)* and development of early markers of mammary carcinogenesis *(34)*. Several studies have shown that the concentration of lignans in the urine of breast cancer patients is lower than in the urine of omnivorous and vegetarian women and of women with low risk of breast cancer *(35–37)*.

Other properties attributed to lignans are the inhibition of cyclic AMP phosphodiesterase *(38)* and fatty acid Δ-5 desaturase activity *(39)*. Lignans are also potent antioxidants in vitro *(13)* and inhibit lipid peroxidation in vivo *(40)*. Therefore, it appears that by reducing oxidative stress they may be important dietary modulators of cancer chemopreventive activity.

We thank G. Schwebel-Schilling for measuring the NMR spectra at 250 MHz, and G. Erben for ESI-MS spectra.

References

1. Keys A, Keys M. How to eat well and stay well, the Mediterranean way. Garden City, UK: Doubleday and Co., 1975:325pp.
2. Keys A, Aravanis C, Van Buchem H, Blackburn H, Buzina R, Djordjevic S, et al. The diet and all-causes death rate in the Seven Countries Study. Lancet 1981;2:58–61.
3. Gerber M. Olive oil and cancer. In: Hill MJ, Giacosa A, Caygill CPG, eds. Epidemiology of diet and cancer. Chichester, UK: Ellis Horwood, 1994:263–75.
4. Hill MJ, Giacosa A. The Mediterranean diet [Editorial]. Eur J Cancer Prev 1992;1:339–40.
5. La Vecchia C, Negri E, Franceschi S, Decarli A, Giacosa A, Lipworth L. Olive oil, other dietary fats, and the risk of breast cancer (Italy). Cancer Causes Control 1998;6:545–50.
6. Martin-Moreno JM, Willett WC, Gorgojo L, Banegas JR, Rodriguez-Artelejo F, Fernandez-Rodriguez JC, et al. Dietary fat, olive oil intake and breast cancer risk. Int J Cancer 1994;58:774–80.
7. Trichopoulou A, Katsouyanni K, Stuver S, Tzala L, Gnardellis C, Rimm E, et al. Consumption of olive oil and specific food groups in relation to breast cancer risk in Greece. J Natl Cancer Inst 1995;87:110–6.
8. Braga C, La Vecchia C, Francheschi S, Negri E, Parpinel M, Decarli A, et al. Olive oil, other seasoning fats, and the risk of colorectal carcinoma. Cancer 1998;82:448–53.
9. Fedeli E. Lipids of olives. Prog Chem Fats Other Lipids 1977;15: 57–74.
10. Fedeli E, Testolin G. Edible fats and oils. In: Spiller GA, ed. The Mediterranean diet in health and disease. New York: Van Nostrand Reinhold, 1991:125–34.
11. Flath RA, Forrey RR, Guadagni DG. Aroma components of olive oil. J Agric Food Chem 1973;21:948–52.
12. Yoo YJ, Fedeli E, Nawar WW. The volatile components produced from olive oil by heating. Riv Ital Sostanze Grasse 1988;65: 415–8.
13. Owen RW, Mier W, Giacosa A, Hull WE, Spiegelhalder B, Bartsch H. Phenolic compounds and squalene in olive oils: the concentration and antioxidant potential of total phenols, simple phenols, secoiridoids, lignans and squalene. Food Chem Toxicol 2000;in press.

14. Papadopoulos G, Boskau D. Antioxidant effect of natural phenols on olive oil. J Am Oil Chem 1991;68:669–71.

15. Montedoro G, Servilli M, Miniati E. Simple and hydrolysable phenolic compounds in virgin olive oil. 1. Their extraction, separation, and quantitative and semiquantitative evaluation by HPLC. J Agric Food Chem 1992;40:1571–6.

16. Montedoro G, Servilli M, Baldioli M, Miniati E. Simple and hydrolysable phenolic compounds in virgin olive oil. 2. Initial characterisation of the hydrolysable fraction. J Agric Food Chem 1993;40: 1577–80.

17. Montedoro G, Servilli M, Baldioli M, Selvaggini R, Miniati E, Macchioni A. Simple and hydrolysable phenolic compounds in virgin olive oil. 3. Spectroscopic characterisation of the secoiridoid derivatives. J Agric Food Chem 1993;41:2228–34.

18. Angerosa F, d'Alessandro N, Konstantinou P, Di Giacinto L. GC-MS evaluation of phenolic compounds in virgin olive oil. J Agric Food Chem 1995;43:1802–7.

19. Angerosa F, d'Alessandro N, Corana F, Melliero G. Characterisation of phenolic and secoiridoid aglycones present in virgin olive oil by gas chromatography-chemical ionisation mass spectrometry. J Chromatogr 1996;736:193–205.

20. Tsukamoto H, Hisada S, Nishibe S. Lignans from bark of the *Olea* plants, 1. Chem Pharm Bull 1984;32:2730–5.

21. Agrawal PK, Pathak AK. Influence of skeletal alteration of lignans on carbon-13 NMR chemical shifts. Magn Reson Chem 1994;32: 753–73.

22. Davin BD, Bedgar DL, Katayama T, Lewis NG. On the stereoselective synthesis of (+)-pinoresinol in *Forsythia suspensa* from its achiral precursor, coniferyl alcohol. Phytochemistry 1992;31: 3869–74.

23. Kato MJ, Chu A, Davin LB, Lewis NG. Biosynthesis of antioxidant lignans in *Sesamum indicum* seeds. Phytochemistry 1998;47: 583–91.

24. Tsukamoto H, Hisada S, Nishibe S. Lignans from bark of the *Olea* plants, 2. Chem Pharm Bull 1985;33:1232–41.

25. Setchell KDR, Lawson AM, Borriello SP, Harkness R, Gordon H, Morgan DML. Lignan formation in man-microbial involvement and possible roles in relation to cancer. Lancet 1981;2:4–7.

26. Setchell KDR, Lawson AM, Conway E, Taylor NF, Kirk DN, Cooley G, et al. The definitive identification of the lignans *trans*-2,3-bis(3-hydroxybenzyl)-butyrolactone and 2,3-bis(3-hydroxybenzyl)butane-1,4-diol in human and animal urine. Biochem J 1981;197:447–58.

27. Axelson M, Sjövall J, Gustafson BE, Setchell KDR. Origin of lignans in mammals and identification of a precursor from plants. Nature 1982;298:659–60.

28. Kardono LB, Tsauri S, Pezzuto JM, Kinghorn AD. Cytotoxic constituents of the bark of *Plumeria rubra* collected in Indonesia. J Nat Prod 1990;53:1447–55.

29. Hirano T, Fukuoka F, Oka K, Naito T, Hosaka K, Mitsuhashi H, et al. Antiproliferative activity of mammalian lignan derivatives against the human breast carcinoma cell line, ZR-75-1. Cancer Investig 1990;8:592–602.

30. Adlercreutz H, Bannwart C, Wähälä K, Mäkelä T, Brunow G, Hase T, et al. Inhibition of human aromatase by mammalian lignans and isoflavoid phytooestrogens. J Steroid Biochem Mol Biol 1993;44: 147–53.

31. Wang C, Mäkelä T, Hase T, Adlercreutz H, Kurzer MS. Lignans and flavonoids inhibit aromatase enzyme in human preadipocytes. J Steroid Biochem Mol Biol 1994;50:205–12.

32. Thompson LU, Robb P, Serraino M, Cheung F. Mammalian lignan production from various foods. Nutr Cancer 1991;16:43–52.

33. Serraino M, Thompson LU. The effect of flaxseed consumption on the initiation and promotional stages of mammary carcinogenesis. Nutr Cancer 1992;17:153–9.

34. Serraino M, Thompson LU. The effect of flaxseed supplementation on early risk markers for mammary carcinogenesis. Cancer Lett 1991;60:135–42.

35. Adlercreutz H, Fotsis T, Heikkinen R, Dwyer JT, Woods M, Goldin BR, et al. Excretion of the lignans enterolactone and enterodiol and of equol in omnivorous and vegetarian women and in women with breast cancer. Lancet 1982;2:1295–9.

36. Adlercreutz H, Fotsis T, Bannwart C, Wähälä K, Mäkelä T, Brunow G, et al. Determination of urinary lignans and phytoestrogen metabolites, potential antioestrogens and anticarcinogens, in urine of women on various habitual diets. J Steroid Biochem 1986;25:791–7.

37. Ingram D, Sanders K, Kolybaba M, Lopez D. Case-control study of phyto-oestrogens and breast cancer. Lancet 1997;350:990–4.

38. Nishibe S, Tsukamoto H, Hisada S, Nikaido T, Ohmoto T, Sankawa U. Inhibition of cyclic AMP phosphodiesterase by lignans and coumarins of *Olea* and *Fraxinus* barks. Shoyakugaku Zasshi 1986;40:89–94.

39. Shimizu S, Akimoto K, Shinmen Y, Kawashima H, Sugano M, Yamada H. Sesamin is a potent and specific inhibitor of Δ5 desaturase in polyunsaturated fatty acid biosynthesis. Lipids 1991;26:512–6.

40. Kang MH, Mait M, Tsujihara N, Osawa T. Sesamolin inhibits lipid peroxidation in rat liver and kidney. J Nutr 1998;128:1018–22.